Received: 21 April 2016 | Revised: 15 November 2016 | Accepted: 16 November 2016

DOI 10.1002/nbm.3683

WILEY NMR IN BIOMEDICINE

RESEARCH ARTICLE

Metabolic remodeling triggered by salivation and diabetes in major salivary glands

Fernando N. Nogueira[1,2†] | **Rui A. Carvalho**[2,3†]

[1] Department of Biomaterials and Oral Biology, School of Dentistry, University of São Paulo, São Paulo, Brazil

[2] Centre for Functional Ecology, University of Coimbra, Portugal

[3] Department of Life Sciences, Faculty of Sciences and Technology, University of Coimbra, Portugal

Correspondence
R. A. Carvalho, Departamento de Ciências da Vida, Universidade de Coimbra, Calçada Martim de Freitas, 3000-456 Coimbra, Portugal.
Email: carvalho@ci.uc.pt

Funding information
FCT (Portuguese Foundation for Science and Technology), Grant/Award Number: PTDC/EBB-EBI/115810/2009; Rede Nacional de RMN, Grant/Award Number: REDE/1517/RMN/2005; FEDER; Operational Competitiveness Program-COMPETE; FCT

The metabolic profile of major salivary glands was evaluated by ^{13}C nuclear magnetic resonance isotopomer analysis (^{13}C NMR-IA) following the infusion of [U-^{13}C]glucose in order to define the true metabolic character of submandibular (SM) and parotid (PA) glands at rest and during salivary stimulation, and to determine the metabolic remodeling driven by diabetes. In healthy conditions, the SM gland is characterized at rest by a glycolytic metabolic profile and extensive pyruvate cycling. On the contrary, the PA gland, although also dominated by glycolysis, also possesses significant Krebs' cycle activity and does not sustain extensive pyruvate cycling. Under stimulation, both glands increase their glycolytic and Krebs' cycle fluxes, but the metabolic coupling between the two pathways is further compromised to account for the much increased biosynthetic anaplerotic fluxes. In diabetes, the responsiveness of the PA gland to a salivary stimulus is seriously hindered, mostly as a result of the incapacity to burst glycolytic activity and also an inability to improve the Krebs' cycle flux to compensate. The Krebs' cycle activity in the SM gland is also consistently compromised, but the glycolytic flux in this gland is more resilient. This diabetes-induced metabolic remodeling in SM and PA salivary glands illustrates the metabolic need to sustain adequate saliva production, and identifies glycolytic and oxidative pathways as key players in the metabolic dynamism of salivary glands.

KEYWORDS

glycolysis, isotopomer analysis, Krebs' cycle, metabolism, salivary glands, salivary stimulation

1 | INTRODUCTION

Saliva is produced by major [submandibular (SM), parotid (PA) and sublingual (SL)] and minor salivary glands, and plays an important role in oral health.[1,2] In humans, without salivary stimulation, SM glands are responsible for about 60% of saliva produced, whereas PA glands contribute about 35%. On stimulation, the relative contribution of PA glands increases to 50%, whereas that of SM glands drops to 35%. However, as a result of major changes in the total volume of saliva produced, 0.3 mL/min at rest *versus* 1.0 mL/min on stimulation, the overall activities of both glands increase considerably (5.0-fold for PA and 2.0-fold for SM glands). Minor glands and the SL gland contribute the remaining percentages.[3]

The salivary secretion process is well known. Basically, sympathetic stimulation is responsible for the secretion of protein-rich saliva, whereas parasympathetic stimulation is responsible for the secretion of saliva rich in water and electrolytes.[4–6] The total saliva composition is also the result of different contributions from salivary glands, which possess distinct histological and secretory characteristics. Although the SM gland produces a mucous saliva, with high mucin contents, the PA gland produces a serous saliva.[7] Although a wealth of knowledge exists about the salivary secretion process, the metabolism behind it is far from being understood. A single study using salivary gland slices indicated that lactate production is higher in the SM than PA gland, suggesting that the SM gland is glycolytic, whereas the PA gland is more oxidative.[8] Further characterization of these metabolic processes is thus mandatory in order to understand the intimate interplay between gland secretory and metabolic activities. In addition, it is widely known that several diseases could affect salivary gland function and saliva secretion. In particular, diabetes mellitus (DM) has been the focus of

†These authors contributed equally to this work.

Abbreviations used: ALT, alanine aminotransferase; CoA, coenzyme A; D, duplet; DM, diabetes mellitus; F_i, metabolic flux *i*; IPR, isoproterenol; KC, Krebs' cycle; LDH, lactate dehydrogenase; NMR-IA, nuclear magnetic resonance isotopomer analysis; OAA, oxaloacetate; PA, parotid; PC, pyruvate carboxylase; PDA, pyruvate dehydrogenase; Pilo, pilocarpine; PK, pyruvate kinase; Q, quartet; S, singlet; SL, sublingual; SM, submandibular; STZ, streptozotocin; [U-^{13}C]glucose, glucose uniformly enriched with ^{13}C.

many studies using major salivary glands, attempting to elucidate the changes in the activity of some pivotal enzymes of the glycolytic pathway (hexokinase and phosphofructokinase 1) and glycogen (glycogen synthase and glycogen phosphorylase) metabolism.[9–11]

Metabolic analysis using ^{13}C isotopomers[12] by nuclear magnetic resonance (NMR) spectroscopy has proven to be a useful and formidable tool for the analysis of intermediary metabolism *in vivo*,[13,14] *ex vivo*[15–17] and *in vitro*.[18] Through the analysis of the ^{13}C labeling patterns in central metabolic intermediates, on administration of ^{13}C-enriched substrates, it is possible to identify and quantify metabolic pathways.[19] Malaisse et al.[20] performed studies in parotid cells using [1-^{13}C]-, [2-^{13}C]- and [6-^{13}C]glucose and D_2O, and analyzed C2- and C3-deuterated lactic acid production in an attempt to unravel enzyme-to-enzyme tunneling phenomena; however, to the best of our knowledge, no studies using stable isotope tracers have been performed in salivary glands.

In this study, we infused rats with [U-^{13}C]glucose and followed ^{13}C incorporation in key metabolic intermediates to identify the metabolic distinctiveness and dynamics of SM and PA salivary glands of control and diabetic rats at rest and throughout simultaneous sympathetic and parasympathetic stimulations. Within this general objective, we also aimed to characterize the metabolic adjustment that accompanies the transition from non-stimulated to stimulated saliva production, and the metabolic remodeling that is triggered by diabetes in each of these major salivary glands.

2 | MATERIALS AND METHODS

2.1 | Materials

[U-^{13}C]glucose (99%) and D_2O (99.9%) were purchased from Euriso-Top (Parc des Algorithmes, Saint-Aubain, France). Isoproterenol (IPR) and pilocarpine (Pilo) were acquired from Sigma-Aldrich (St. Louis, MO, USA).

2.2 | Animals

Male Wistar-Han rats were used in this study. At 8 weeks of age, two groups were formed: control (n = 10) and diabetic (n = 10). DM was induced by a single intraperitoneal injection of streptozotocin (STZ) (60 mg/kg body weight) dissolved in 0.1 mol/L citrate buffer, pH 4.5. The progress of DM was confirmed by blood glucose analysis, using the blood glucose meter Accu Chek Advantage (Roche-Diagnostics, Basel, Switzerland), 48 h after STZ injection, in overnight fasted animals. Rats with a blood glucose level greater than 14 mM (>250 mg/100 mL) were considered to be diabetic.

Rats were group-housed in type III-H cages (Tecniplast, Bizerte, Tunisia) and maintained in climate-controlled facilities with free access to standard chow and water. At 12 weeks, the control and diabetic animals were further subdivided. Thus, four groups of animals were used in the infusion protocols defined below: control at rest (n = 5) and control stimulated (n = 5); diabetic at rest (n = 5) and diabetic stimulated (n = 5).

All animals were handled in accordance with the guidelines of Ethical Principles of Animal Experimentation adopted by COBEA. The Protocol of this study was approved by the Ethical Committee for Animal Research of the School of Dentistry of the University of São Paulo (protocol 16/2014).

2.3 | Stable isotope tracer infusion

[U-^{13}C]glucose, dissolved in saline (0.5 g/mL), was administered to anesthetized (mixture of ketamine–xylazine, 50: 20 mg/kg body weight) animals [for a duration of 3 h using an infusion pump (11 Plus infusion pump, Harvard Apparatus Holliston, MA, USA)]. The total infusion time of 3 h was chosen as a compromise between the need to achieve considerable enrichments in salivary glands and the requirement to keep infusion periods within acceptable limits. An initial bolus (60 mg/kg) was given to allow faster appearance of significant levels of [U-^{13}C]glucose in plasma. After this, a constant rate of glucose infusion was used (2.5 μL/min). Salivary gland stimulation was achieved using a single dose of IPR (5 mg/kg) and Pilo (1 mg/kg) administered intraperitoneally 2 h after the start of infusion. At the end of the 3 h of infusion, animals were sacrificed, and SM and PA glands were surgically removed and freeze clamped with aluminum tongs pre-cooled in liquid nitrogen.

Glands were extracted in perchloric acid using previously described procedures.[16] Briefly, pulverized gland tissue was added to ice-cold 6% perchloric acid (2 vol/g wet tissue) and stirred vigorously. After centrifugation (3000 ***g***), the supernatant was neutralized with ice-cold KOH solution, causing the precipitation of $KClO_4$. The supernatant, containing all aqueous soluble metabolites, was lyophilized and re-dissolved in 200 μL of a D_2O (99.9%) phosphate-buffered (pD 7.0, 100 mM) solution containing 10 mM sodium fumarate, used as internal standard.

2.4 | ^{1}H and ^{13}C NMR analyses

^{1}H and ^{13}C NMR spectra of extracts were acquired on a 14.1-T VNMRS spectrometer (Varian, Palo Alto, CA, USA) equipped with a 3-mm broadband NMR probe.

Each ^{1}H NMR spectrum consisted of 65k points defining a 7.2-kHz spectral width, and 64 scans were averaged to ensure adequate signal-to-noise ratios. A 30° radiofrequency observe pulse and an interpulse delay of 10 s were used to ensure full relaxation of proton magnetization.

Each ^{13}C NMR spectrum consisted of 131k points defining a 37-kHz spectral width. A 45° radiofrequency observe pulse and an interpulse delay of 3 s were used to ensure full relaxation of all aliphatic carbons in the sample. Averaged scans varied between 10k and 20k to ensure adequate signal-to-noise ratios for ^{13}C multiplet quantification.

Spectral deconvolution for quantitative analysis was performed using NUTSpro™ NMR software (Acorn NMR Inc., Livermore, CA, USA).

2.5 | Metabolic pathways

Figure 1A shows a schematic representation of the monitored metabolic pathways. The infused tracer, [U-^{13}C]glucose, enters the salivary glands and is metabolized through several metabolic pathways. Flux F_1 denotes total glucose consumption. Through the analysis of the ^{13}C labeling patterns of central metabolic intermediates, we can infer the

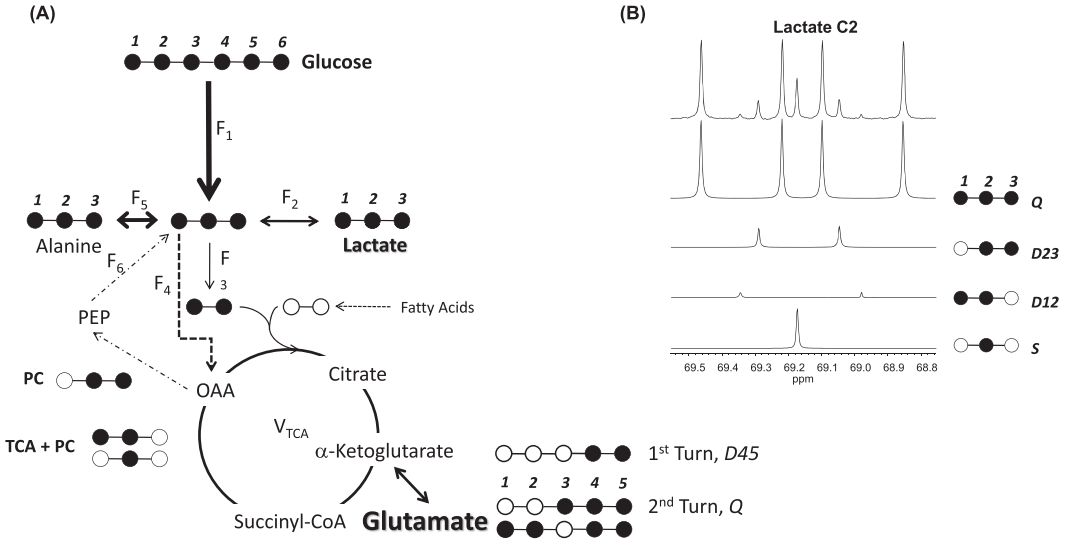

FIGURE 1 A, Schematic representation of the metabolic pathways (F_1–F_6) involved in the metabolism of [U-^{13}C]glucose: F_1, glycolysis; F_2, lactic fermentation; F_3, acetyl-CoA synthesis by pyruvate dehydrogenase (PDH); F_4, oxaloacetate synthesis by pyruvate carboxylase (PC); F_5, alanine synthesis by alanine aminotransferase (ALT); F_6, pyruvate cycling by pyruvate kinase (PK). OAA, oxaloacetate; PEP, Posphoenolpyruvate TCA, Tricarboxylic Acid Cycle or Krebs Cycle. B, Lactate C2 multiplet analysis provides information concerning four distinct lactate isotopomers originating from various metabolic pathways (see text for details). Glutamate C4 multiplet analysis provides information on the extent of Krebs' cycle turnover

prevalence of specific metabolic fluxes in any given experimental condition: (i) flux F_2 refers to the lactic fermentation pathway, in which pyruvate is converted into lactate by lactate dehydrogenase (LDH) with the regeneration of NAD^+ to sustain glycolysis; (ii) flux F_3 refers to the oxidative flux through the Krebs' cycle, prompted by pyruvate dehydrogenase (PDH) activity; (iii) flux F_4 represents anaplerotic flux through pyruvate carboxylase (PC); (iv) flux F_5 denotes the fast equilibrium between the α-ketoacid pyruvate and alanine, catalyzed by alanine aminotransferase (ALT); (v) flux F_6 indicates pyruvate cycling as a result of pyruvate kinase (PK) activity. From the analysis of the prevalence of specific ^{13}C isotopomers of metabolic intermediates, it is possible to determine the kinetics of glycolytic and Krebs' cycle fluxes, the metabolic coupling between the two metabolic pathways and the involvement of anaplerosis, pyruvate cycling and Krebs' cycle turnover.

2.6 | Lactate ^{13}C NMR isotopomer analysis

Lactate derived from [U-^{13}C]glucose is uniformly enriched ([U-^{13}C]lactate) if derived directly from glycolytic pyruvate, whereas other labeling patterns imply the activity of specific metabolic pathways: (i) pyruvate cycling (F_6) by itself, which generates [2,3-$^{13}C_2$]lactate directly; (ii) following one turn of the Krebs' cycle, which forms [1,2-$^{13}C_2$]- and [3-^{13}C]lactate; (iii) following two turns of the Krebs' cycle, which forms [1-$^{13}C_2$]- and [2-^{13}C]lactate. The lactate C2 resonance allows the distinction of these metabolic contributions, as [U-^{13}C]- forms a quartet (Q), [2,3-$^{13}C_2$]- a doublet (D23), [1,2-$^{13}C_2$]- another doublet (D12), with distinct ^{13}C–^{13}C scalar coupling, and [2-^{13}C]lactate a singlet (S), which will add to the natural abundance contribution (Figure 1B).

2.7 | Glutamate ^{13}C NMR isotopomer analysis

[1,2-$^{13}C_2$]acetyl-CoA, generated from [U-^{13}C]pyruvate, can be fully oxidized in the Krebs' cycle, leading to the appearance of [4,5-$^{13}C_2$]α-ketoglutarate, which exchanges with glutamate, thus forming [4,5-$^{13}C_2$]glutamate. This isotopomer appears in the carbon 4 resonance as a doublet (D45). By following the cycle, this labeling pattern generates oxaloacetate (OAA) with two alternative labeling patterns, [1,2-$^{13}C_2$]- or [3,4-$^{13}C_2$]OAA. These, by condensation with another [1,2-$^{13}C_2$]acetyl-CoA, allow the appearance of multi-labeled Krebs' cycle intermediates and, subsequently, [3,4,5-$^{13}C_3$]- and [1,2,4,5-$^{13}C_4$]glutamate are formed. The isotopomer [3,4,5-$^{13}C_3$]glutamate appears in the carbon C4 resonance as a doublet of doublets or pseudo-quartet (Q), and is an indicator of the extent of Krebs' cycle turnover (Figure 1A).

2.8 | Cytosolic redox ratios

An indirect measure of cytosolic [$NADH/H^+$]/[NAD^+] is given by the ratio between lactate and alanine. In conditions of high cytosolic $NADH/H^+$ contents, LDH activity reduces pyruvate levels and, concomitantly, alanine levels.[21] Higher tissue contents of lactate relative to both pyruvate and alanine are also consistent with a lesser dependence on oxidative flux through the Krebs' cycle and an increased prevalence of anaplerotic fluxes, distinctive of highly biosynthetic tissues.

2.9 | Statistical analysis

Statistical analysis of the different results was performed using Minitab 16 software (State College, PA, USA). employing Student' *t*-test. A significance of 5% was considered for all comparisons.

3 | RESULTS

3.1 | ^{1}H NMR analysis of salivary gland metabolites

Figure 2A shows a representative ^{1}H NMR spectrum of a perchloric acid extract from a PA gland of a control animal at rest. Major

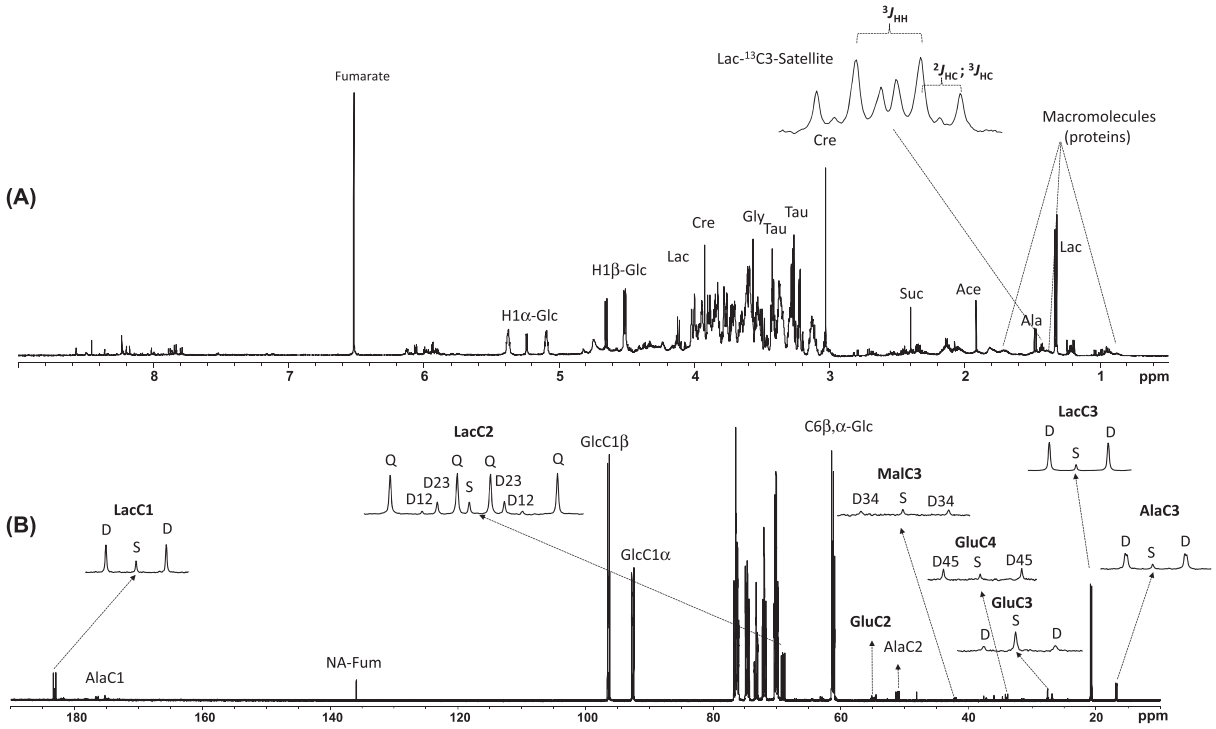

FIGURE 2 14.1-T ^{1}H (A) and ^{13}C (B) NMR spectra of a perchloric acid extract from a parotid (PA) gland. Major metabolites are identified in the ^{1}H NMR spectrum (Ace, acetate; Ala, alanine; Cre, creatine; Glc, glucose; Gly, glycine; Lac, lactate; Suc, succinate; Tau, taurine), together with an expansion of the methyl ^{13}C satellite caused by the lactate originating from [U-^{13}C]glucose, which appears as a duplet of triplets as a result of homonuclear ($^{3}J_{HH}$) and heteronuclear ($^{2}J_{HC}$, $^{3}J_{HC}$) scalar couplings. The ^{13}C multiplets for multiple resonances and metabolites are expanded in the ^{13}C NMR spectrum to elucidate the concept of ^{13}C NMR isotopomer analysis of tissue extracts: alanine carbon 3, AlaC3; glutamate carbon 3, GluC3; glutamate carbon 4, GluC4; lactate carbon 1, LacC1; lactate carbon 2, LacC2; lactate carbon 3, LacC3; malate carbon 3, MalC3

metabolites are identified, including several resonances caused by glycoproteins (broader resonances), unlabeled lactate (doublet, 1.33 ppm) and labeled lactate (multiplet, 1.40 ppm), alanine (doublet, 1.45 ppm), acetate (singlet, 1.9 ppm), succinate (singlet, 2.37 ppm), creatine (singlet, 3.0 ppm) and fumarate (singlet, 6.5 ppm; internal reference). The expansion represents one of the lactate ^{13}C satellites and comprises several lactate ^{13}C isotopomers (see Materials and Methods).

Figure 3 (top) shows the expansions of ^{1}H NMR spectra from extracts of SM (left) and PA (right) glands for control and diabetic animals. SM (A) and PA (B) glands have distinct metabolite profiles, with the levels of acetate, succinate and glycoproteins being significantly higher in the SM gland. In control animals, on stimulation, a significant increase in lactate content, mostly from unlabeled (^{12}C) origin, is observed in both SM (C) and PA (D) glands and, in PA glands, such stimulation causes a significant reduction in acetate and succinate levels.

A comparison between controls and diabetic animals shows that ^{1}H NMR spectra from diabetic animals at rest have higher acetate levels in SM glands (E) and higher lactate levels in PA glands (F). With salivary stimulation, the acetate levels in SM glands (G) are considerably decreased, whereas there is no significant alteration in PA glands (H) compared with the rest condition.

Ratios of unlabeled lactate to alanine (Lac/Ala) were determined from ^{1}H NMR spectra, and are essentially identical to those calculated using the ^{13}C NMR spectra, presented in Figure 4 (LacC3F/AlaC3F), indicating that PA glands have higher ratios than SM glands under control conditions, and that stimulation increases these ratios significantly in both SM and PA glands. In diabetic animals, the ratios are identical in SM glands, both at rest and on stimulation, but considerably higher than in controls in PA glands at rest. Stimulation in diabetic PA glands has no effect on these ratios.

3.2 | ^{13}C NMR analysis of salivary gland metabolites

Figure 2B shows the ^{13}C NMR spectrum from the perchloric acid extract from a PA gland of a control animal. Several metabolites are identified and expansions from their resonances are described in terms of their ^{13}C multiplets. The most abundant metabolites are lactate (LacC3, 20.8 ppm; LacC2, 69.1 ppm), alanine (AlaC3, 17.0 ppm; AlaC2, 51.2 ppm) and glutamate (C3-Glu, 27.6 ppm; C4-Glu, 34.2 ppm; C2-Glu, 55.5 ppm).

Ratios of LacC3 to AlaC3 (LacC3F/AlaC3F) were determined (Figure 4) and, in control animals, increase significantly in both SM and PA glands on stimulation. Stimulation in diabetic animals also increases this ratio in SM glands, but PA glands fail to respond.

The expansions of LacC2 (Figure 3, bottom) show a complex multiplet pattern that can be associated with specific metabolic fluxes (see Materials and Methods). Changes in the relative contributions of each multiplet to the overall LacC2 resonance are easily noticeable between gland types (SM *versus* PA), animal groups (control *versus* diabetic) and secretory states (rest *versus* stimulated). Pyruvate cycling, indicated by the presence of the multiplet D23, is more pronounced at rest in SM than in PA glands, and stimulation causes a significant reduction only in SM glands. Krebs' cycle activity, given by the increase above natural abundance in the S component and the appearance of D12, is

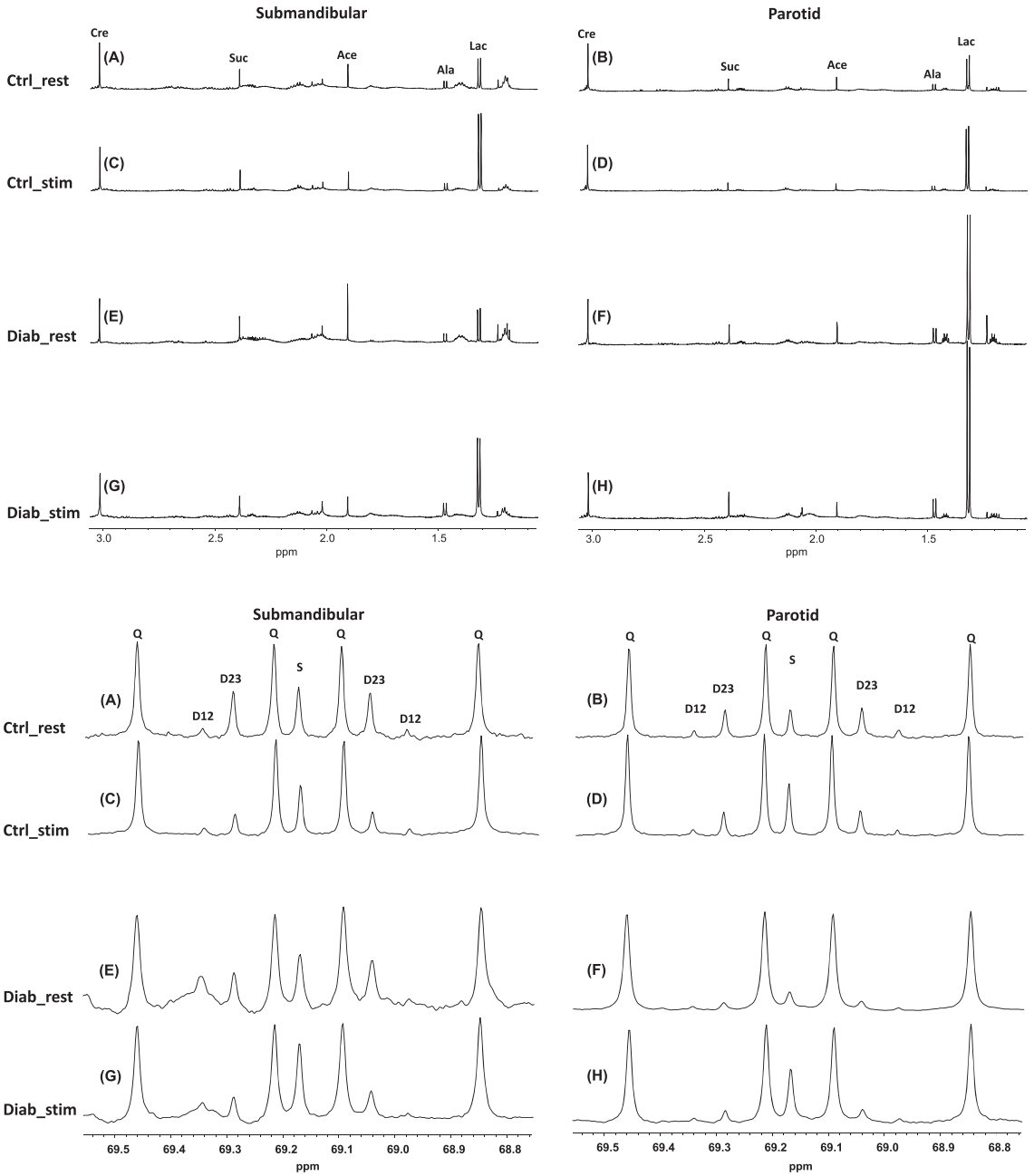

FIGURE 3 Top: expansions of the aliphatic regions (1.05–3.05 ppm) from the ^{1}H NMR spectra of tissue perchloric acid extracts. Control animals at rest: submandibular (SM) (A) and parotid (PA) (B). Stimulated control animals: SM (C) and PA (D). Diabetic animals at rest: SM (E) and PA (F). Stimulated diabetic animals: SM (G) and PA (H). Major metabolites include lactate (Lac), alanine (Ala), acetate (Ace), succinate (Suc) and creatine (Cre). Bottom: expansions of lactate C2 (LacC2) resonances from the ^{13}C NMR spectra of tissue perchloric acid extracts. Control animals at rest: SM (A) and PA (B). Stimulated control animals: SM (C) and PA (D). Diabetic animals at rest: SM (E) and PA (F). Stimulated diabetic animals: SM (G) and PA (H). The multiplets are identified as follows: quartet (Q), from uniformly ^{13}C-enriched lactate; doublet 23 (D23), from lactate ^{13}C-enriched in carbons 2 and 3; doublet 12 (D12), from lactate ^{13}C-enriched in carbons 1 and 2; singlet (S), from lactate singly ^{13}C-enriched

significantly reduced on stimulation in SM glands from controls, but remains essentially unaltered in PA glands from controls and in both SM and PA glands from diabetic animals (Figure 4).

An analysis of the GluC4 resonances shows that, in control animals at rest, SM glands possess a lower contribution of the D45 multiplet (GluC4D) relative to that in diabetic animals, and that stimulation induces a significant increase in this multiplet in SM glands from control animals and a significant reduction in SM glands from diabetic animals. No significant differences are noticeable for this multiplet in PA glands in all experimental conditions (Figure 4).

The GluC3F/GluC4F ratios were also evaluated and show no significant reductions in either SM or PA gland after stimulation, and also no interference caused by diabetes. The enrichment in glutamate carbon C3 is of multiple origins, including Krebs' cycle turnover and anaplerosis through PC, rendering the interpretation of this ratio quite complex, particularly under non-steady-state metabolic conditions. Nevertheless, the comparison was made and the absence of differences helps our understanding of the mechanisms of metabolic remodeling when combined with other metabolic data. Finally, the LacC3F/GluC4F ratio shows only a significant increase in PA glands at rest from diabetic animals relative to controls.

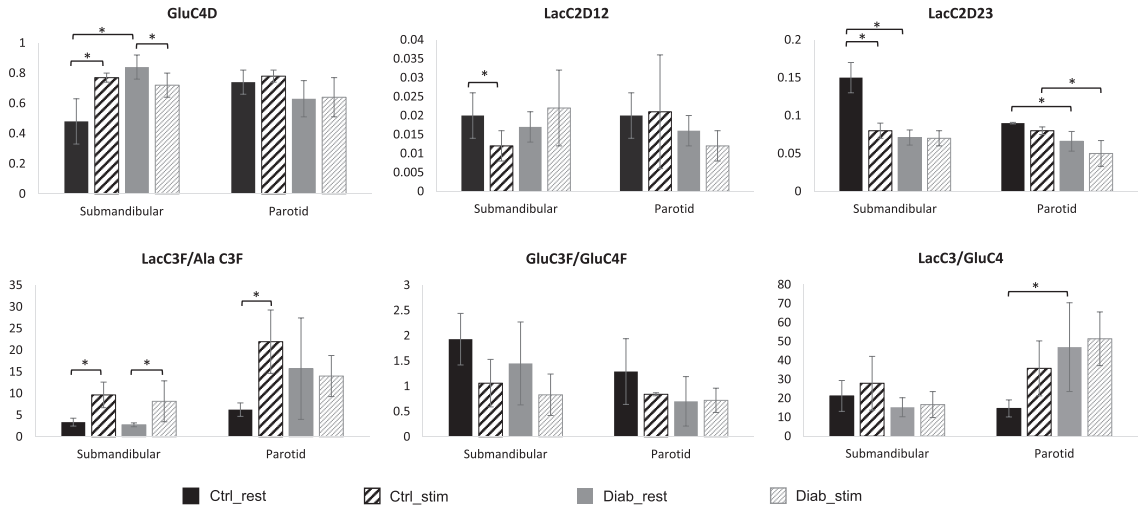

FIGURE 4 Metabolic parameters derived from the analysis of ^{13}C NMR spectra of submandibular (SM) and parotid (PA) glands from control and diabetic animals at rest and stimulated: ratio of ^{13}C-lactate to ^{13}C-alanine (LacC3F/AlaC3F), using carbon 3 of each metabolite; doublet 12 in lactate carbon 2 multiplet (LacC2D12); doublet 23 in lactate carbon 2 multiplet (LacC2D23); doublet in carbon 4 of glutamate caused by simultaneous ^{13}C enrichment in carbons 4 and 5 (GluC4D); ratio of full (F) ^{13}C enrichment between carbons 3 and 4 of glutamate (GluC3F/GluC4F). *Statistical significance ($p < 0.05$) between the assigned groups

4 | DISCUSSION

Salivary glands produce and secrete high quantities of saliva and this process is highly dependent on both the availability of energy and substrates for biosynthesis. SM and PA glands account, by themselves, for approximately 90% of total saliva, both at rest and on stimulation. However, the relative contributions of these glands are different under different physiological states. The salivary composition from these glands is also very different as a consequence of their distinct histological and secretory characteristics.

An understanding of the metabolic fundamentals of these very important organs is of paramount importance in the determination of their function in various pathologies[3] which undermine saliva production and affect the overall quality of life of patients. Some information exists concerning the general glycolytic and oxidative characters of major glands.[8,22] Unfortunately, it is very limited in terms of the dynamic character of such metabolic pathways and their overall involvement in the physiological process. In this study, and for the first time, a ^{13}C NMR isotopomer analysis was performed *in vivo* in order to determine: (i) the occurrence of glycolysis and Krebs' cycle fluxes in SM and PA glands, both at rest and on stimulation, and the key metabolic characters of each gland; (ii) the degree of coupling between the two above-mentioned pathways and its response driven by stimulation; (iii) the importance of anaplerotic pathways in the whole metabolic dynamics of salivary glands; (iv) the metabolic reworking that occurs in each gland as a function of a disease that is known to be associated with significant alterations in the salivary secretory process.

A ^{1}H NMR analysis of tissue extracts provided information concerning the abundance of major metabolites and a method to determine the cytosolic redox potential at rest and on stimulation. The LacC3F/AlaC3F ratios determined for control animals show a more oxidized cytosol in SM (2.9 ± 0.8) than in PA (5.3 ± 1.2) glands and an enormous increase in cytosolic redox on stimulation in both SM (10.0 ± 2.9) and PA (15.7 ± 3.3) glands. This increased redox state on stimulation is strongly correlated with increased glycolysis in both glands and is typical of tissues with a high biosynthetic activity.[23] Although, at rest, PA glands are less required than SM glands for the process of saliva secretion, they still need considerable energy to produce stocks, provided by both glycolysis and the Krebs' cycle. On stimulation, the burst in PA gland activity requires further energy, which could derive from both increased glycolysis and Krebs' cycle activity. An analysis of this ratio in SM and PA glands from diabetic animals shows essentially identical behavior to that found in controls in SM glands and the absence of responsiveness to salivary stimulation by PA glands. At rest, the PA glands of diabetic animals are characterized by high levels of lactate and, on stimulation, no significant alteration is detected in terms of both lactate levels and LacC3F/AlaC3F ratios. This incapacity to respond to salivary stimulation is apparently not present in SM glands, suggesting that the diabetic condition affects more considerably the PA glands, at least from this cytosolic redox perspective.

Levels of acetate and succinate (Figure 3, top) are also very variable and are related to Krebs' cycle activity. Increased levels of both metabolites are frequently associated with a truncated Krebs' cycle and indicate a metabolic state essentially unrelated to oxidative activity. In control animals, the levels of these two metabolites are relatively higher in SM than in PA glands, denoting a higher dependence on glycolysis at rest in SM glands. On stimulation, no significant changes can be seen in succinate and acetate in SM glands but, in PA glands, a decrease in these metabolites is evident. This more perceptible reduction in PA glands is consistent with the increased demand on the function of these glands after salivary stimulation,[3] and helps us to understand the importance of the Krebs' cycle in PA gland metabolism. In diabetic animals, the levels of succinate and acetate are higher than in controls, in both SM and PA glands, and both at rest and on stimulation. In particular, acetate levels are significantly increased in SM

glands at rest, suggesting a further hampering of Krebs' cycle activity in these glands caused by the diabetic condition. On stimulation, however, SM glands show substantially reduced acetate levels, clearly demonstrating the readiness of the SM glands from diabetic animals to respond to salivary stimulation. The sensitivity of the PA glands seems to be rather reduced, although some reduction in acetate levels occurs on salivary activation.

The combination of the ^{1}H NMR data on lactate levels, lactate/alanine ratios and concentrations of succinate and acetate allow an estimation of the general sensitivity of the glands to salivary stimulation and permit the correlation of such sensitivity with the promptness to activate glycolysis and Krebs' cycle fluxes. Diabetes appears to be characterized by a loss of metabolic awareness, which is particularly pronounced in PA glands, and is characterized by a near-elimination of the glycolytic burst and a sizeable inhibition in Krebs' cycle activity.

The ^{1}H NMR spectra also show higher contents of glycoproteins in SM relative to PA glands (Figure 3, top), in accordance with the typical high glycoprotein composition of saliva from SM glands.[24] On stimulation, the intracellular concentration of this glycoprotein is considerably reduced as a result of increased saliva secretion.

All the above findings on unlabeled metabolites are very robust in terms of 'static' metabolic analysis, but very limited in their capacity to analyze the dynamics of the metabolic fluxes and their interrelationships, which can only be scrutinized by tracer methodologies.[19] In this study, the tracer of choice was [U-^{13}C]glucose because of the uniqueness of the ^{13}C labeling patterns of metabolic intermediates after metabolization and the sensitivity to complex metabolic pathways (branched pathways).

Isotopomer analysis of tissue lactate allows the measurement of the extent of involvement of lactic acid fermentation (F_2) relative to pathways such as pyruvate cycling (F_6) and the Krebs' cycle. Shuffling of carbons in each pathway confers distinctive ^{13}C labeling patterns easily distinguished by ^{13}C NMR analysis. C2 of lactate appears as a distinctive nine-line multiplet (S + D12 + D23 + Q) and is distinct among experimental groups (Figures 1B and 3, bottom). The Q multiplet, obtained from glycolytically derived [U-^{13}C]lactate, is more abundant than any other multiplet, in both SM and PA glands at rest and on stimulation, consistent with the essential role of glycolysis followed by lactic acid fermentation (F_2) in these glands (Figure 3, bottom). The LacD23 multiplet is more pronounced when pyruvate cycling (F_6) is more active. Active pyruvate 'futile' cycling is synonymous of tissue 'biosynthetic attentiveness'. In SM glands from control animals, salivary stimulation of LacD23 is reduced to accommodate the extra requirements of biosynthetic intermediates; however, in diabetic animals, no alterations in the level of this multiplet are realized, denoting the low predominance of this pathway in overall gland metabolism. In PA glands, there is a significant difference between controls and diabetic animals, but stimulation does not seem to play any major role in PA gland metabolism, as suggested by the absence of alterations in LacD23. The LacD12 multiplet is small under all circumstances and denotes the activity of the Krebs' cycle followed by pyruvate cycling. In SM glands from control animals at rest, because of higher pyruvate cycling and lower Krebs' cycle activity, this isotopomer shows more abundantly, whereas, on stimulation, both the reduced pyruvate cycling and the increased Krebs' cycle contribute to a significant reduction in this doubly labeled isotopomer ([1,2-^{13}C]lactate) (Figure 4) in favor of the singly labeled ([2-^{13}C]lactate) form, given by the singlet (S), because of tracer dilution (Figure 3, bottom). This could result from an increased contribution of non-enriched endogenous glycogen[25–27] and non-enriched fatty acids[28] to the acetyl-CoA pool feeding the Krebs' cycle on stimulation. For the SM glands in diabetic animals and PA glands in control and diabetic animals, no significant reductions in LacD12 are detectable, again reflecting a lesser involvement of the Krebs' cycle pathway in the overall metabolism of PA glands and glands from diabetic animals.

By measurement of the LacC3F/GluC4F ratio, we can chart the metabolic coupling between glycolysis and the Krebs' cycle. Improved coupling between these metabolic pathways prompts higher enrichment in GluC4 as a result of LacC3 oxidation, and is seen as a ratio reduction. In contrast, the ratio increases if there is an imbalance between lactate production and oxidation, resulting either from Krebs' cycle inhibition or glycolysis stimulation without concurrent Krebs' cycle activation. Fine tuning between these two metabolic processes determines the true metabolic character of each gland. SM and PA glands present similar coupling at rest, although the high ratios (>10) suggest an extensive glycolytic character for both glands, but more prominent in PA glands. On stimulation, the biosynthetic needs are increased in both SM and PA glands, accentuating the need for carbon biosynthetic blocks, further stretching the glycolytic dependence and metabolic character. A more pronounced uncoupling in PA glands from diabetic animals is also comprehensible considering the poorer contribution of the Krebs' cycle to gland metabolism.

In previous studies by our group, we observed a greater commitment of SM salivary glands than PA glands in carbohydrate metabolism in the diabetic state.[28] All of these enzymatic studies were performed on tissues extracted from animals at rest, without any type of stimulation. The results presented in this study for stimulated SM glands, in control and diabetic animals, further emphasize the importance of SM glands in sustaining adequate salivary function. As the SM gland is the major gland responsible for mucin secretion at rest, a protein related to the viscous capacity of saliva, the reduction in Krebs' cycle activity in the diabetic state leads to a reduction in mucin secretion, consistent with our previous findings using diabetic rats with minimally stimulated saliva secretion.[29]

Major conclusions from this study are depicted in the scheme presented in Figure 5. The metabolic dynamics between glycolysis, the Krebs' cycle and pyruvate cycling fluxes that characterize SM (Figure 5A) and PA (Figure 5B) glands at rest and SM (Figure 5C) and PA (Figure 5D) glands on salivary stimulation are significantly disturbed by diabetes. Under control conditions, salivary stimulation bursts glycolytic activity, mainly associated with endogenous glycogen clearance, and the Krebs' cycle is also considerably activated, but resorts to non-glycolytic unlabeled carbon sources. Overall, the diabetic condition causes metabolic disturbances that hinder the glands from performing their ordinary saliva secretion, which include, essentially, an inhibition of glycolysis responsiveness in PA glands and, to a lesser extent, a smaller involvement of Krebs' cycle activity compared with controls.

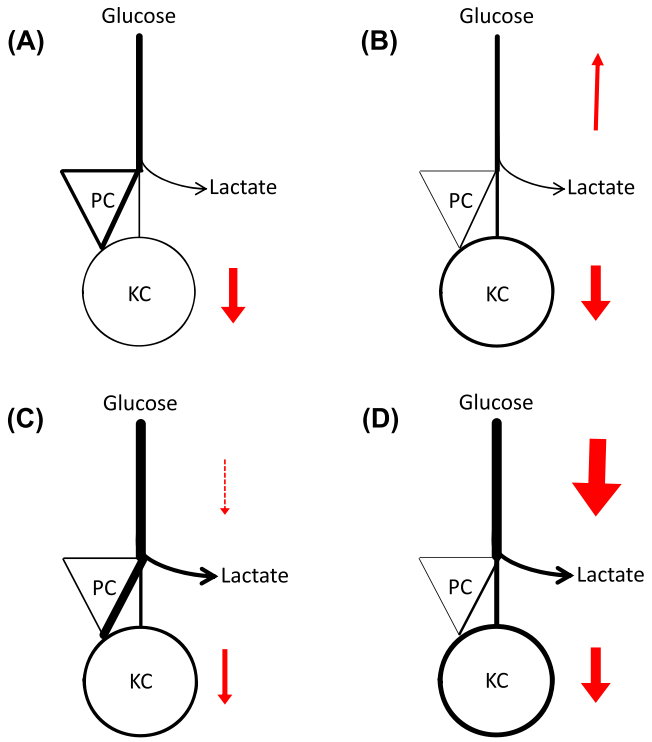

FIGURE 5 Schematic representation of the metabolic remodeling taking place in submandibular (SM) and parotid (PA) glands on stimulation. Glycolytic and Krebs' cycle (KC) coupling, lactate production and pyruvate cycling (PC) interplay are shown: SM (A) and PA (B) glands at rest, and SM (C) and PA (D) glands on stimulation. Red arrows depict changes in flux prompted by diabetes. Line thickness correlates with metabolic flux activity and arrow thickness with the level of the effect of diabetes on the metabolic flux

ACKNOWLEDGEMENTS

FNN acknowledges Coordenação de Aperfeiçoamento de Pessoal de Nível Superior (CAPES) for a post-doctoral fellowship (Processes BEX 17665/12-4) and financial support from Project 88881.062183/2014-01. RAC acknowledges FCT (Portuguese Foundation for Science and Technology) for financial support (Grant: PTDC/EBB-EBI/115810/2009). We also acknowledge the 'Rede Nacional de RMN' (REDE/1517/RMN/2005) for access to their facilities. This work was funded by Fundo Europeu de Desenvolvimento Regional (FEDER) Funds through the Operational Competitiveness Program-COMPETE and by National Funds through FCT under the project FCOMP-01-0124-FEDER-020970 (PTDC/QUI-BIQ/120319/2010).

CONFLICT OF INTEREST

There are no conflicts of interest to declare.

REFERENCES

1. Dodds MW, Johnson DA, Yeh CK. Health benefits of saliva: a review. *J Dent*. 2005;33(3):223–233.
2. Sreebny LM. Saliva in health and disease: an appraisal and update. *Int Dent J*. 2000;50(3):140–161.
3. Edgar WM, Dawes C, O'Mullane DM. *Saliva and Oral Health*. Bicester, UK.: Stephen Hancocks Limited; 2012.
4. Proctor GB, Carpenter GH. Regulation of salivary gland function by autonomic nerves. *Auton Neurosci*. 2007;133(1):3–18.
5. Vatta MS, Hope SI, Prendes GM, Bianciotti LG, Elverdin JC, Fernandez BE. Salivary glands and noradrenergic transmission in diabetic rats. *Auton Autacoid Pharmacol*. 2002;22(2):65–71.
6. Melvin JE, Yule D, Shuttleworth T, Begenisich T. Regulation of fluid and electrolyte secretion in salivary gland acinar cells. *Annu Rev Physiol*. 2005;67:445–469.
7. Nanci A. *Ten Cate's Oral Histology: Development, Structure, and Function*. Amsterdam: Mosby Elsevier; 2008.
8. Nicolau J, Sassaki KT. Metabolism of carbohydrate in the major salivary glands of rats. *Arch Oral Biol*. 1976;21(11):659–661.
9. Nogueira FN, Santos MF, Nicolau J. Influence of streptozotocin-induced diabetes on hexokinase activity of rat salivary glands. *J Physiol Biochem*. 2005;61(3):421–427.
10. Nicolau J, Souza DN, Nogueira FN. Activity, distribution and regulation of phosphofructokinase in salivary gland of rats with streptozotocin-induced diabetes. *Braz Oral Res*. 2006;20(2):108–113.
11. Nicolau J, de Matos JA, de Souza DN, Neves LB, Lopes AC. Altered glycogen metabolism in the submandibular and parotid salivary glands of rats with streptozotocin-induced diabetes. *J Oral Sci*. 2005;47(2):111–116.
12. London RE. C-13 labeling in studies of metabolic-regulation. *Prog Nucl Mag Res Sp*. 1988;20:337–383.
13. Henry PG, Oz G, Provencher S, Gruetter R. Toward dynamic isotopomer analysis in the rat brain in vivo: automatic quantitation of ^{13}C NMR spectra using LCModel. *NMR Biomed*. 2003;16(6–7):400–412.
14. Mason GF, Rothman DL. Basic principles of metabolic modeling of NMR (13)C isotopic turnover to determine rates of brain metabolism in vivo. *Metab Eng*. 2004;6(1):75–84.
15. Chance EM, Seeholzer SH, Kobayashi K, Williamson JR. Mathematical-analysis of isotope labeling in the citric-acid cycle with applications to C-13 Nmr-studies in perfused rat hearts. *J Biol Chem*. 1983;258(22):3785–3794.
16. Carvalho RA, Rodrigues TB, Zhao P, Jeffrey FM, Malloy CR, Sherry AD. A (13)C isotopomer kinetic analysis of cardiac metabolism: influence of altered cytosolic redox and [Ca(2+)](o). *Am J Physiol Heart Circ Physiol*. 2004;287(2):H889–H895.
17. Malloy CR, Thompson JR, Jeffrey FM, Sherry AD. Contribution of exogenous substrates to acetyl coenzyme A: measurement by ^{13}C NMR under non-steady-state conditions. *Biochemistry*. 1990;29(29):6756–6761.
18. Vega-Naredo I, Loureiro R, Mesquita KA, et al. Mitochondrial metabolism directs stemness and differentiation in P19 embryonal carcinoma stem cells. *Cell Death Differ*. 2014;21(10):1560–1574.
19. Wolfe RR, Chinkes DL. *Isotope Tracers in Metabolic Research: Principles and Practice of Kinetic Analysis*. Hoboken: John Wiley & Sons Canada; 2004.
20. Malaisse WJ, Biesemans M, Sener A, Willem R. ^{13}C NMR study of C2- and C3-deuterated lactic acid production by parotid cells exposed to ^{13}C-labeled glucose in the presence of D_2O. *Biochem Med Metab Biol*. 1994;53(1):67–74.
21. Williamson DH, Lund P, Krebs HA. The redox state of free nicotinamide-adenine dinucleotide in the cytoplasm and mitochondria of rat liver. *Biochem J*. 1967;103(2):514–527.
22. Nicolau J, Lansac MC, Rosa R, Pedroso FI, Leal A. Activities of some glycolytic enzymes in the major salivary glands of some laboratory animals. *Comp Biochem Physiol A*. 1974;47(2):399–402.
23. Morrish F, Isern N, Sadilek M, Jeffrey M, Hockenbery DM. c-Myc activates multiple metabolic networks to generate substrates for cell-cycle entry. *Oncogene*. 2009;28(27):2485–2491.
24. Carpenter GH. The secretion, components, and properties of saliva. *Annu Rev Food Sci Technol*. 2013;4:267–276.
25. Nicolau J, Sassaki KT. Metabolism of carbohydrate in vitro of the submandibular salivary glands (SMG) from mice injected with isoproterenol. *Gen Pharmacol*. 1983;14(6):705–708.

26. Herman G, Rossignol B. Regulation of protein secretion and metabolism in rat salivary glands. Effects of norepinephrine and carbachol on the glycogenolysis in submaxillary glands. *Eur J Biochem/FEBS*. 1975;55(1):105–110.
27. Garrett JR, Thomopoulos GN, Zhang XS, Hartley R. The fate of glycogen in granular tubule cells of rat submandibular glands during secretory events. *Arch Oral Biol*. 1994;39(5):449–452.
28. Anderson LC, Garrett JR. Lipid accumulation in the major salivary glands of streptozotocin-diabetic rats. *Arch Oral Biol*. 1986;31(7):469–475.
29. Romero AC, Ibuki FK, Nogueira FN. Sialic acid reduction in the saliva of streptozotocin induced diabetic rats. *Arch Oral Biol*. 2012;57(9):1189–1193.

How to cite this article: Nogueira FN, Carvalho, RA. Metabolic remodeling triggered by salivation and diabetes in major salivary glands. *NMR in Biomedicine*. 2017;30:e3683. doi: 10.1002/nbm.3683